

Spatio-Temporal Availability in Satellite-to-Indoor Broadcasting

Marko Milojević¹, Giovanni Del Galdo¹, Nuan Song¹, Martin Haardt¹, Albert Heuberger²

¹*Communications Research Laboratory, Ilmenau University of Technology*

P.O. Box 100565, 98684 Ilmenau, Germany, Phone: + 49 (3677) 69-2673, Fax: + 49 (3677) 69-1195
 { marko.milojevic, giovanni.delgaldo, nuan.song, martin.haardt}@tu-ilmenau.de

²*Fraunhofer Institute Integrierte Schaltungen IIS*

Am Wolfsmantel 33, 91058 Erlangen, Germany
 albert.heuberger@iis.fraunhofer.de

Abstract— This contribution studies the spatio-temporal availability of satellite links inside typical indoor environments. The spatio-temporal satellite-to-indoor channels are obtained by a 3D ray tracing engine and by a geometry-based channel modeling tool. In this paper the temporal fluctuations of the channels have been modeled based on satellite-to-indoor measurements. Here the performance of single as well as multiple receive antennas with different polarimetric radiation patterns are compared for different satellite elevation angles. The results show that additional antennas placed at the receiver reduce both the spatial and temporal variability of the received power, leading to a significant reduction in transmit power necessary for the same target availability.

I. INTRODUCTION

Satellite broadcasting systems are very attractive due to a possible coverage of large areas. For the planning of satellite communication systems, the characterization of the propagation environment is of significant importance. Some satellites, such as XM Radio, offer link margins of up to 18 dB which makes indoor reception already feasible. For future satellite systems, a significant increase of the Effective Isotropic Radiated Power (EIRP) is planned, which will allow indoor reception of the satellite signals with reasonably high availability for broadband services.

To characterize the satellite-to-indoor channels, either measured channels or channels obtained by deterministic channel models such as ray-tracers can be analyzed. In the literature, only a few measurements are discussed dealing with the performance of different receive antenna strategies, polarization diversity, and the influence of moving persons or objects. Measurement results in [1] show that the received electromagnetic field is strongly diffused in the interior of a building. Therefore, the received power does not depend on either the gain function or the polarization of different types of antennas. In [2] it is concluded that the wall attenuation has the highest influence on the indoor coverage in the range of 1.1 GHz - 1.6 GHz. Within the MAESTRO project [3], [4], satellite-to-indoor measurements in the L-band have been carried out in Erlangen and Athens by using the Worldspace Afristar satellite having an EIRP of 48 dBW. It is concluded that the percentage of positions where a satellite signal can be received with good quality lies in the range of 30 % up to 80 % with

corresponding link margins of 10 to 16 dB. In [5], it is shown that the polarization state of the propagation wave changes significantly inside the room.

In this paper we extend the investigations carried out in [6] with respect to the temporal variation, elevation, and to more antenna configurations by means of analyzing MAESTRO measurement data. This paper is organized as follows: in Section II we describe our deterministic channel modeling concept. Then, in Section III we analyze the measurements to acquire information on the temporal variations of the channel. Finally, in Section IV, we discuss the influence of different antenna configurations, polarizations, elevations, and temporal variations of the channel on the satellite-to-indoor link availability for realistic link margins. In Section V we draw the conclusions.

II. THE SATELLITE-TO-INDOOR DETERMINISTIC CHANNEL MODEL

The satellite-to-indoor channel coefficients are obtained by using the 3D ray-tracing simulation tool WinProp [7] to obtain the information on the propagation paths and the IImProp [8], a flexible geometry-based MIMO channel modeling tool for wireless communications developed at Ilmenau University of Technology, to create the channels for various antenna configurations. Moreover, temporal variation of the receive power is also taken into account. WinProp takes into account transmission, reflection, and diffraction. In [9], [10], and [11] WinProp has been validated with the help of measurements. After the satellite-to-indoor scenario is defined and modeled by the WinProp tool, the path strength and spatial information of each path obtained from WinProp is fed to the IImProp. In particular, the trajectory of each path is modeled by means of point-like scatterers which represent points of interaction. The IImProp, by supporting different receive antenna patterns, allows us to study receive diversity. A circularly polarized satellite signal with carrier frequency 2.0 GHz is received by a stationary indoor receiver. Reflections and diffractions can change the polarization of the waves. In [1] and [5], it is concluded that in the satellite-to-indoor scenario the electromagnetic field is diffuse and the circular polarization is not preserved in the far field away from the window. Therefore,

in the IImProp simulation step, a random polarization state is given to each multi-path component, while the LOS is set to be Left Hand Circular Polarized (LHCP). In [6], more details on the deterministic channel modeling components can be found.

III. TEMPORAL VARIATION OF THE SATELLITE LINK

If the satellite receiver position and transmit EIRP are fixed, the received signal strength will vary on the small scale only due to the movement of the objects in the vicinity of the receiver: some propagation paths disappear while others appear, leading to either destructive or constructive interference. Such variations of the received power are usually caused by:

- A man moving between the satellite and the receive antenna.
- A man moving in the vicinity of the receive antenna, but not being between the satellite and the receive antenna.
- Movements of the objects such as trees or cars between the satellite and the receiver.

It is reported in [3] that the movement of a tree blocking the satellite signal increases the standard deviation of the signal in time by 0.8 dB and that the body blocking the incoming signal increases the attenuation by additional 7 - 13 dB.

We have analyzed the MAESTRO measurements [3] with and without person movement around the receiver. The person movement, without blocking the incoming signal, increases the received signal variance in all available data sets. The standard deviation increases in the range from 0.7 dB up to 1.2 dB, depending on the environment. We have also analyzed the Probability Density Function (PDF) of the difference between the received power in measurements with and without person movement. The PDF is well approximated by the PDF of a truncated Gaussian function with zero mean and standard deviation in the range from 0.7 dB up to 1.5 dB, depending on the environment. In Figure 1, the PDF of the measurement difference and the fitted truncated Gaussian curve are shown. The latter has zero mean, a standard deviation of 0.8 dB, and truncation at ± 2.3 dB.

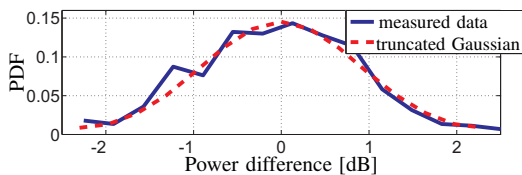


Fig. 1. PDF of the difference between the received power with and without person moving (no signal blockage)

IV. SIMULATION RESULTS

For the simulation results presented here we consider man movement around the receiver without blocking the receive signal. This effect is modeled by the truncated Gaussian PDF introduced in the previous section.

In our studies we consider a room oriented towards the satellite, i.e., there is LOS between the satellite and the window. The carrier-to-noise ratio at the receiver, denoted by C/N , is defined as the difference between the received signal

power C and the received noise power N , i.e., $C/N = C - N$, expressed in dB.

The value of the Fade Depth FD is defined as the difference between a reference carrier-to-noise ratio C/N_{ref} and the carrier-to-noise ratio at the receiver C/N , i.e., $FD = (C/N_{\text{ref}} - C/N)$ dB, where C/N_{ref} refers to a position outside of the room in a pure LOS regime.

The Link Margin LM is defined as the difference between the reference carrier-to-noise ratio C/N_{ref} and the minimum carrier-to-noise ratio C/N_{min} needed for good reception of the signal, i.e., $LM = (C/N_{\text{ref}} - C/N_{\text{min}})$ dB. If the fade depth is higher than the link margin we say that the communication link is *not available*, otherwise it is *available*.

Figure 2 shows the predicted receive signal power in the room for a satellite elevation of 40° and an azimuth φ of 45° . With respect to the receive signal power, as seen in Figure 2,

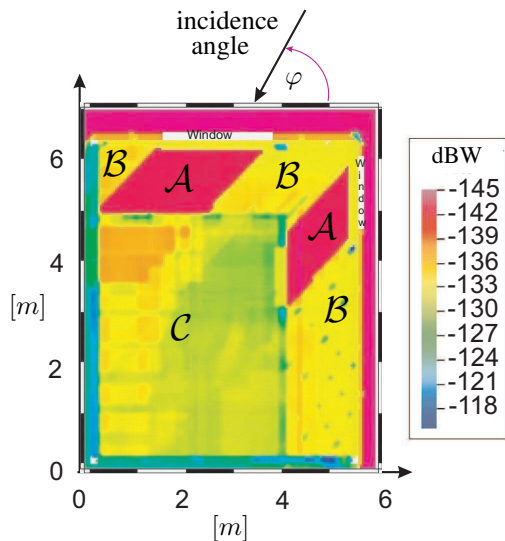


Fig. 2. Average receive power in dBW simulated by WinProp

three areas in the room can be distinguished:

- The area \mathcal{A} is dominated by the path impinging directly through the window. The fade depth is low and exhibits very low spatial variation. Therefore, a very high availability is achieved.
- The area \mathcal{B} is characterized by rays impinging through the walls. The received power is significantly lower than in area \mathcal{A} , while the spatial variation of the signal power is higher.
- In the area \mathcal{C} most of the signal power arrives after penetration through the wall or window followed by some reflections and diffractions. The spatial variation is higher than in areas \mathcal{A} and \mathcal{B} .

The WinProp has been used to obtain the information on the incoming signal components with a resolution of 8 cm in the room. For each point, the IImProp uses this information to produce the channel impulse responses in a window of size $2\lambda \times 2\lambda$ by using a Uniform Rectangular Array (URA) of size 16×16 , resulting in 256 subchannels. Finally, temporal variation modeled by a truncated Gaussian distribution, as described

in Section III, is included. The aim of the simulations is to assess the possible improvements of the spatio-temporal signal availability when different receive antenna configurations are used, namely: one vertically polarized dipole antenna (V), two displaced vertically polarized dipoles (V-V), four displaced vertically polarized dipoles (4-V), one vertically and one horizontally polarized dipole antennas placed at the same position (V-H), two displaced vertically and two horizontally polarized dipole antennas (V-H-V-H). Similarly to the vertical dipoles, we consider 1, 2, and 4 circularly polarized antennas, denoted by (C), (C-C), and (4-C), respectively. The radiation patterns of the considered antennas are shown in Figure 3.

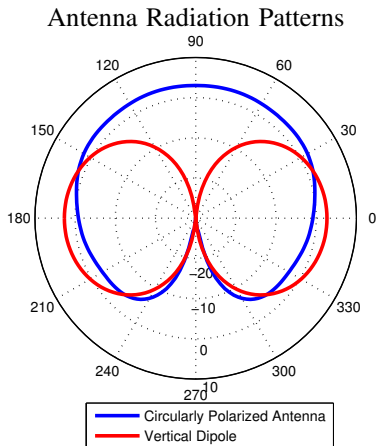


Fig. 3. Antenna patterns vs. elevation. The patterns are symmetric with respect to the vertical axis and the values are expressed in dBi.

The distance between adjacent antenna elements is set to a quarter of the wavelength. Maximum Ratio Combining (MRC) is assumed at the receiver. The transmitted signal is left hand circularly polarized. The penetration losses of the window, brick walls, and the concrete ceiling are 2 dB, 12 dB, and 17 dB, respectively. In Figure 4, the correlation coefficients between different antenna types within area \mathcal{A} and within area \mathcal{C} are depicted, and in Figure 5 the Cumulative Distribution Function (CDF) of the fade depth within the whole room is shown. The correlation coefficient determines the diversity gain and the antenna array gain: whereas high values of the correlation coefficient lead to a high array gain, low values lead to a high diversity gain. In the area \mathcal{A} all correlation coefficients have very high values that drop slowly when the distance between antennas is increased. In the area \mathcal{C} the correlation coefficient between two circularly polarized closely spaced antennas is higher than for two vertically or two horizontally polarized antennas with the same separation. Moreover, the correlation coefficient between one vertically polarized and one horizontally polarized antenna within area \mathcal{C} is very low for all antenna distances. The correlation coefficient within the area \mathcal{A} is significantly higher than in the area \mathcal{C} for all antenna configurations.

The combination of circularly polarized antennas offer the best availability in area \mathcal{A} (corresponds to the low CDF region

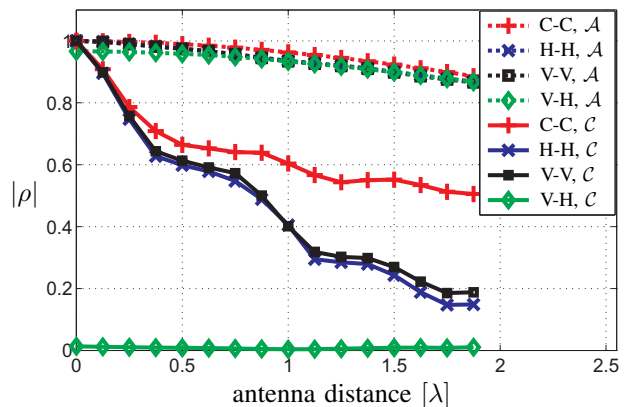


Fig. 4. Correlation coefficients between different antenna types within area \mathcal{A} and \mathcal{C} separately

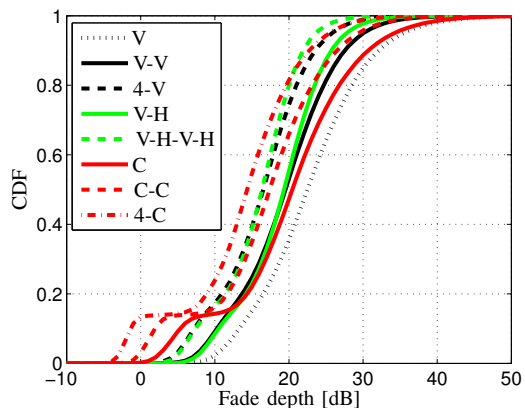


Fig. 5. Cumulative distribution function of the fade depth. The satellite elevation is 40° , and the transmitted signal is LHCP.

in Figure 5) since they have the same polarization as the transmitted signal and the highest gain at an elevation of 40° . Moreover, the signals between two or more circularly polarized antennas are highly correlated, introducing an additional array gain at low CDF values. In high availability regimes (region of high CDF values) in Figure 5 the best performance is achieved with the use of the V-H-V-H array. At an availability of 99%, it has a 3 dB gain over the 4-V and 4-C array, and a 7 dB gain over the C-C scheme. This is a result of the very low correlation coefficient of the V-H-V-H scheme and the fact that the diversity gain increases with higher availability. It is known from the literature [3] that the link margin of 15 dB in existing systems is realistic. For this link margin in our investigation the highest availability of 55% is achieved with the 4-C array, while the C-C, V-H-V-H and 4-V antenna configurations have availabilities close to 30%. For the antenna configuration C-C, the availability within area \mathcal{A} equals 100%, within area \mathcal{B} approximately 39%, and within area \mathcal{C} 10%. Obviously, the best place to put the receiver is just behind the windows, anywhere within area \mathcal{A} . Three possible straightforward ways to increase the availability are: 1) increase of the number of antenna elements, 2) considering

the possibility that the user is willing to test the reception at different positions, and 3) a combination of the first two approaches. In the scenarios we studied, an availability of 50% can be achieved with the use of 4 circularly polarized antennas (4-C), or, equivalently, by randomly testing a single circularly polarized antenna receiver at 4 different positions. In the near future, satellites with higher EIRP will be available, leading to higher link margins. The target availability will be close to 100%. In that case the best receive antenna choice at an elevation of 40° would be the combination of vertically and horizontally polarized receive antennas due to the low correlation of the received signals in the area C .

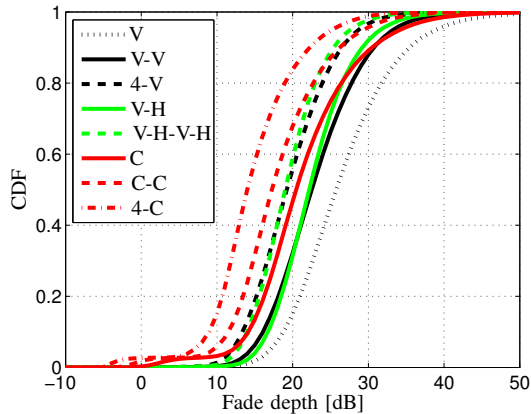


Fig. 6. Cumulative distribution function of the fade depth. The satellite elevation is 70° , and the transmitted signal is LHCP.

At higher elevations the size of the area A decreases. Therefore, in these cases, the steep increase of the CDF for lower values of the fade depth (between 0 and 5 dB) is strongly reduced. The CDF of the fade depth for a satellite elevation of 70° is depicted in Figure 6. For all elevations and antenna distances, the correlation coefficient between one horizontally and one vertically polarized antenna is very close to zero. The correlation coefficients between two horizontally (H-H) and two circularly polarized antennas (C-C) decrease for higher satellite elevations. Moreover, the difference between these two correlations also decreases. Therefore, the diversity gain difference between antenna configurations with the same number of elements in middle and high areas of the corresponding CDF of the fade depth is reduced. Additionally, the radiation pattern of the circularly polarized antenna at an elevation of 70° is higher than radiation patterns of vertically or horizontally polarized dipoles. Therefore, the antenna arrays consisting of circularly polarized antennas outperform other antenna arrays with an equal number of antenna elements at higher elevations for all CDF values.

The temporal variation of the received power presented in Section III influences the link margin needed to provide a target availability. While at medium availabilities, e.g., 50%, man shadowing has almost no influence, at high availabilities the link margin should be increased up to 0.6 dB for one antenna receivers to neglect the influence of the temporal variation on availability. If a four antenna receiver is con-

sidered, this value drops to 0.15 dB, due to the diversity. If the broadcasting system supports time interleaving and channel coding, the influence of the channel temporal variation becomes negligible.

V. CONCLUSIONS

This paper presents the results of studies on the spatio-temporal availability in satellite-to-indoor broadcasting communications. The study is carried out on the basis of a 3D ray tracing engine and of a geometry-based channel modeling tool, combined with the evaluation of measurements. Various antenna configurations at the receiver with different polarimetric radiation patterns are compared. Additional antennas placed at the receiver reduce the spatio-temporal variability of the channel, leading to a better performance of the system. In the LOS areas, the best performance is achieved by multiple circularly polarized receive antennas. On the other hand, in the NLOS areas, a combination of horizontally and vertically polarized antennas is a good candidate, especially if very high availabilities are considered. The temporal changes due to a person movement in the vicinity of the receiver can be modeled by a truncated Gaussian function. Its influence grows with an increase of the target availability. Our simulations have shown that it can be neglected if time interleaving and channel coding are supported by the system, which is usually the case.

REFERENCES

- [1] B. G. Molnár, I. Frigyes, Z. Bodnár, Z. Herczku, Zs. Kormányos, J. Bérces, I. Papp, and L. Juhász, "A detailed experimental study of the LEO satellite to indoor channel characteristics," *International Journal of Wireless Information Networks*, April 1999.
- [2] F. Pérez-Fontán, B. Sanmartín, A. Steingaf, A. Lehner, J. Selva, E. Kubista, and B. Arbesser-Rastburg, "Measurements and modeling of the satellite-to-indoor channel for Galileo," in *European Navigation Conference GNSS 2004*, Rotterdam, The Netherlands, May 2004.
- [3] T. Heyn and C. Wagner, "Propagation channel characterisation - Final report," IST Integrated Project No 507023 Ú MAESTRO, Jan. 2005.
- [4] T. Heyn, A. Heuberger, and C. Keip, "Propagation measurements for the characterisation of a hybrid mobile channel in s-band," in *Proc. IST Mobile Summit Conference*, Dresden, Germany, June 2005.
- [5] L. Farkas and L. Nagy, "Satellite-to-indoor wave propagation channel simulation. First results - the polarization characteristics of the indoor wave," *Personal, Indoor and Mobile Radio Communications, PIMRC'2000*, Sept. 2000.
- [6] N. Song, G. Del Galdo, M. Milojević, M. Haardt, and A. Heuberger, "Spatial availability in satellite-to-indoor broadcasting communications," in *Proc. 7th Workshop Digital Broadcasting*, Erlangen, Germany, Sept. 2006, pp. 113–118.
- [7] "http://www.awe-communications.com," .
- [8] G. Del Galdo, M. Haardt, and C. Schneider, "Geometry-based channel modelling of MIMO channels in comparison with channel sounder measurements," *Advances in Radio Science - Kleinheubacher Berichte*, pp. 117–126, October 2003.
- [9] G. Wölfle, B. E. Gschwendtner, and F. M. Landstorfer, "Intelligent ray tracing - A new approach for the field strength prediction in microcells," *47th Vehicular Technology Conference (VTC) 1997*, May 1997.
- [10] R. Hoppe, T. Hager, T. Heyn, A. Heuberger, and H. Widmer, "Simulation and measurement of the satellite to indoor propagation channel at L- and S-band," in *Proc. EuCAP 2006*, France, Nice, Nov. 2006.
- [11] G. Wölfle, R. Hoppe, and F. M. Landstorfer, "A fast and enhanced ray optical propagation model for indoor and urban scenarios, based on an intelligent preprocessing of the database," in *Proceedings of the 10th IEEE International Symposium on Personal, Indoor and Mobile Radio Communications (PIMRC)*, Osaka, Japan, Sept. 1999.